

Supporting Information

(D)_n-σ-(A)_m Type Partially Conjugated Block Copolymer and its Performance in Single-Component Polymer Solar Cells

Dae Hee Lee, Ji Hyung Lee, Hyung Jong Kim, Suna Choi, Gi Eun Park, Min Ju Cho* and Dong Hoon Choi*

Dept. of Chemistry, Research Institute for Natural Sciences, Korea University, 5 Anam-dong, Sungbuk-gu, Seoul 136-701, Korea

Measurement: The ¹H-NMR spectra were recorded using a Bruker 500 MHz spectrometer (Ascend™ 500, Bruker) in deuterated chloroform purchased from Cambridge Isotope Laboratories, Inc. (Andover, MA, USA). A Thermo Scientific Flash 2000 (Thermo Fisher Scientific) elemental analyzer was used to determine the content of C, H, N and S. The molecular weights of the polymers were determined by gel permeation chromatography (GPC, Agilent GPC 1200 series) using a polystyrene standard in *o*-dichlorobenzene (*T* = 80 °C) as the eluent.

Matrix-assisted laser desorption ionization time of flight (MALDI-TOF) mass spectrometry (LRF20, a Bruker Daltonics) was measured to confirm the structure of monofunctionalized P4 (Fig. S8). Sample was prepared by spotting the chloroform solution with matrix on the target plate. 2-Hydroxy-1-naphthoic acid was used for the matrix.

To study the UV-visible absorption behavior, we prepared thin film samples of the polymers on glass substrates as follows. A chloroform solution (1 wt.%) of each polymer was filtered through an Acrodisc syringe filter (Millipore 0.45 μm , Millipore, Billerica, MA, USA) and subsequently spin-cast on glass. The absorption spectra of the samples as thin films and as solutions (chloroform, conc. 1×10^{-5} mol L⁻¹) were obtained using a UV-Vis absorption spectrometer (Agilent 8453, photodiode array, $\lambda = 190\text{--}1100$ nm). Photoluminescence (PL) spectra were recorded with a Hitachi F-7000 fluorescence spectrophotometer at room temperature.

The thermal properties of the polymers were studied under a nitrogen atmosphere on a Mettler 821^e differential scanning calorimeter (DSC) (Mettler, Greifensee, Switzerland). The redox properties of the polymers were examined by cyclic voltammetry (CV) (EA161 eDAQ). The polymer thin films were coated on a Pt plate using chloroform. The electrolyte solution was 0.10 M tetrabutylammonium hexafluorophosphate (Bu_4NPF_6) in freshly dried acetonitrile. Ag/AgCl and Pt wire (0.5 mm in diameter) electrodes were used as the reference electrode and the counter electrode, respectively. The scan rate was 20 mV s⁻¹.

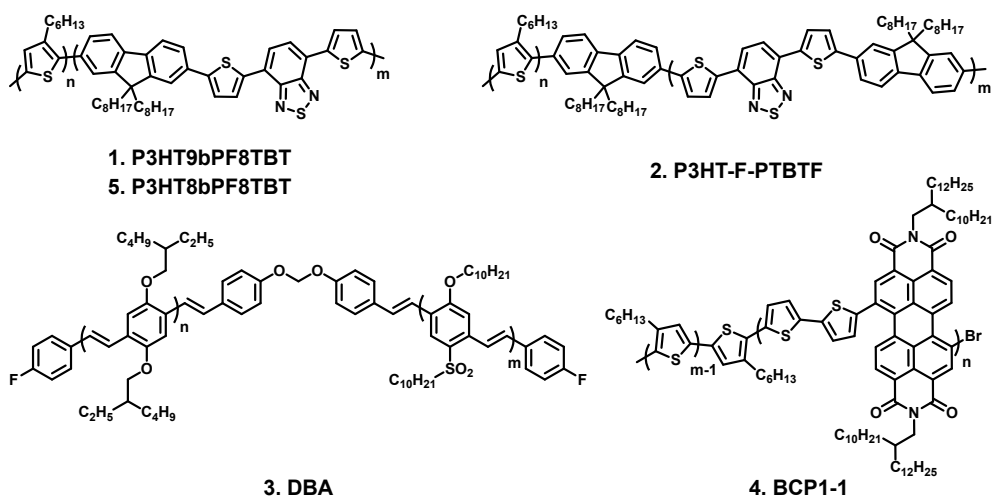
Grazing-incidence wide-angle X-ray scattering (GIWAXS) measurements were performed at the 9A (U-SAXS) beamline (energy = 11.17 keV, pixel size = 79.6 μm , wavelength = 1.110 \AA , at the Pohang Accelerator Laboratory (PAL)). The measurements were obtained over a scanning interval of 2ϑ between 0 and 20°. The variables q_{xy} and q_z are the components of the scattering vector parallel and perpendicular to the substrate, respectively, where $q = (4\pi/\lambda) \sin \vartheta$. λ is the wavelength of the incident radiation, and ϑ is equal to half the scattering angle. The film samples were fabricated by spin-coating the polymer solutions on OTS-treated silicon wafers (OTS-SiO₂/Si), followed by drying at 50 °C under vacuum.

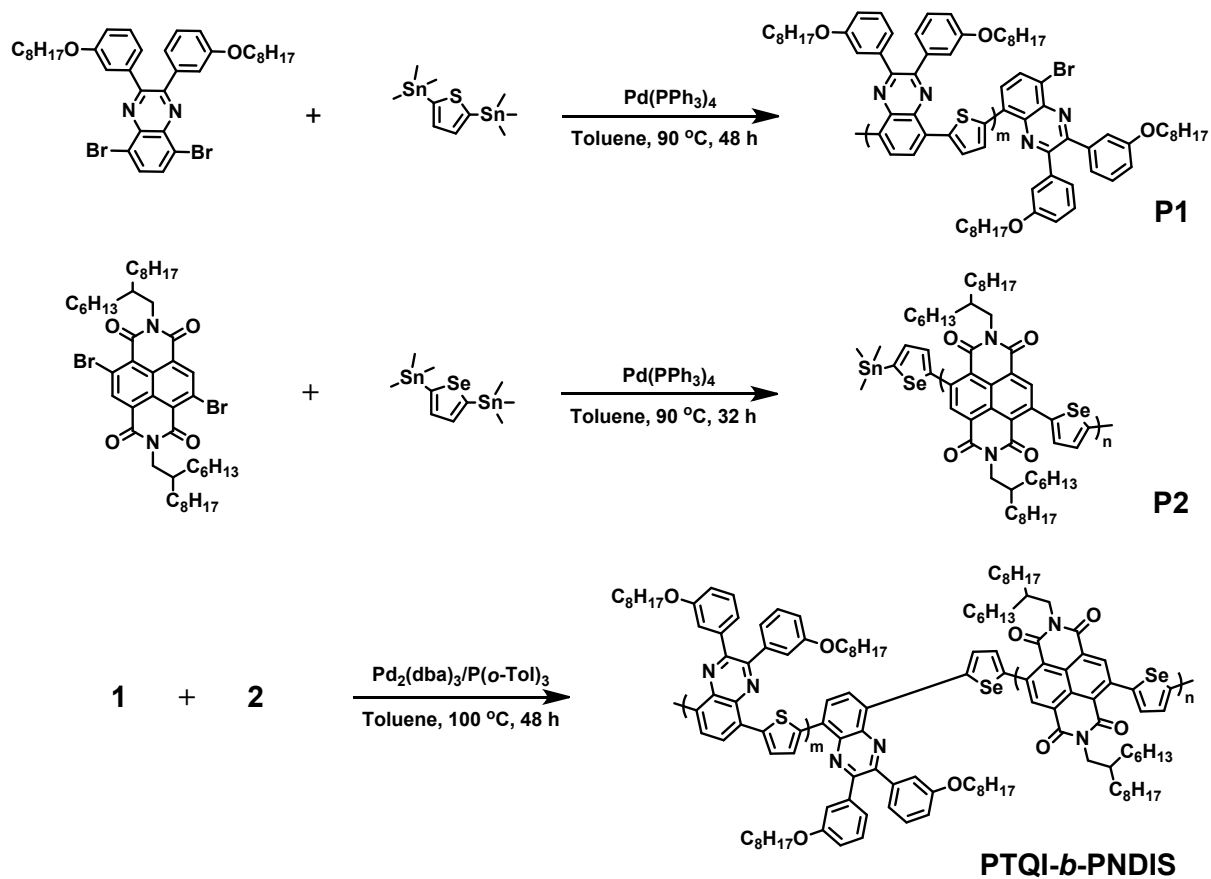
Atomic force microscopy (AFM, Advanced Scanning Probe Microscope, XE-100, PSIA) in tapping mode with a silicon cantilever was used to characterize the surface morphology of the polymer films. The film samples were fabricated by spin-coating (2000 rpm) onto an OTS-treated or untreated silicon wafer followed by drying at 50 °C under vacuum (Solvent: chloroform, solution conc.: 10 mg mL⁻¹). The AFM images of the polymer films for OPV were obtained from the thin films fabricated by spin-coating the chloroform solution on the ZnO layer on ITO glass. Transmission electron microscopy (TEM) imaging was performed using a Tecnai G2F30 transmission electron microscope (FEI Inc.; accelerating voltage = 300 kV). The corresponding samples were prepared by coating the blend solution on a carbon-coated copper grid.

Table S1. Summary of the PSC performance progress with single active component using block copolymers

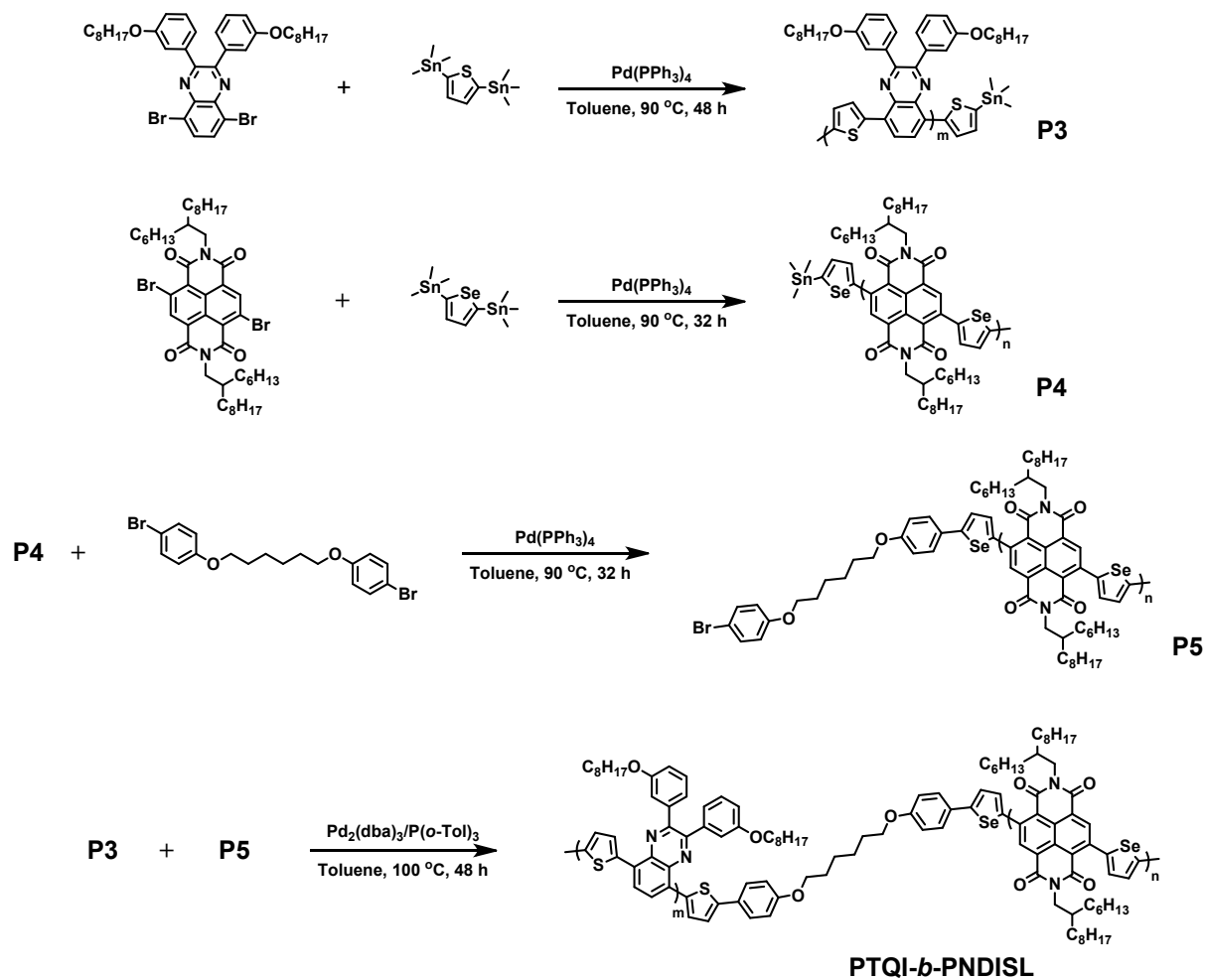
Entry	Material	Thermal annealing	Solvent additive	J_{sc} (mA cm ⁻²)	V_{oc} (V)	FF (%)	PCE (%)	Ref.
1	P3HT-b-PFTBT	165 °C 20 min	-	3.1	1.10	26	0.91	25
2	P3HT-F-PTBTF	165 °C 15 min	CN ^a 5 vol%	4.73	1.11	42	2.24	26
3	DBA	-	-	0.92	0.65	26	0.2	27
4	BCP1-1	150 °C 10 min	-	5.29	0.43	43	1.00	28
5	P3HT8bPF8TBT	165 °C 10 min	-	5.2	1.23	47	3.1	30

^a chloronaphthalene





Scheme S1. Synthetic scheme for PTQI-*b*-PNDIS.



Scheme S2. Synthetic scheme for PTQI-*b*-PNDISL.

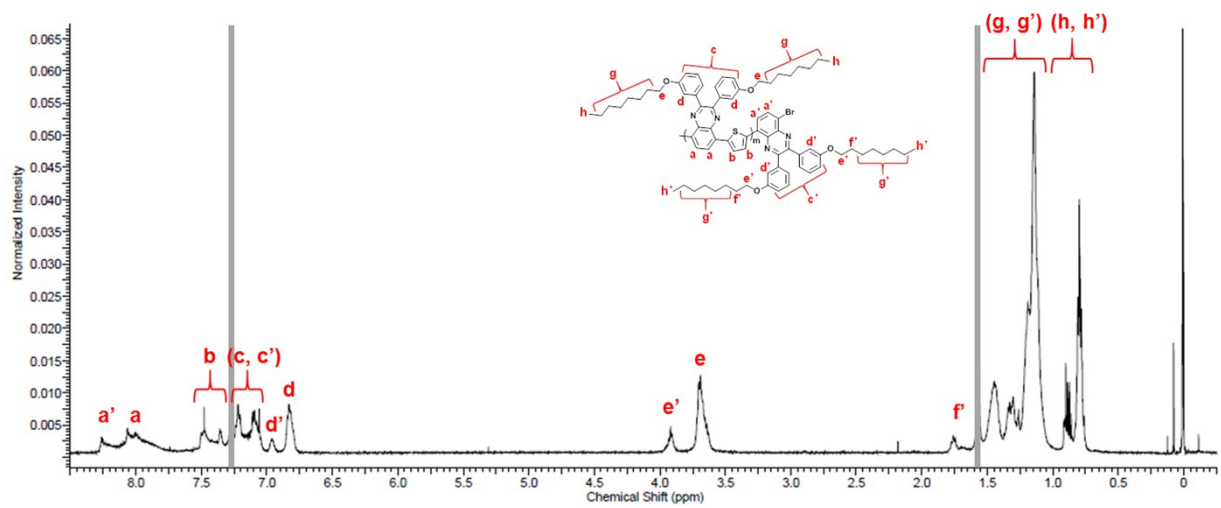


Fig S1. ^1H NMR spectrum of P1.

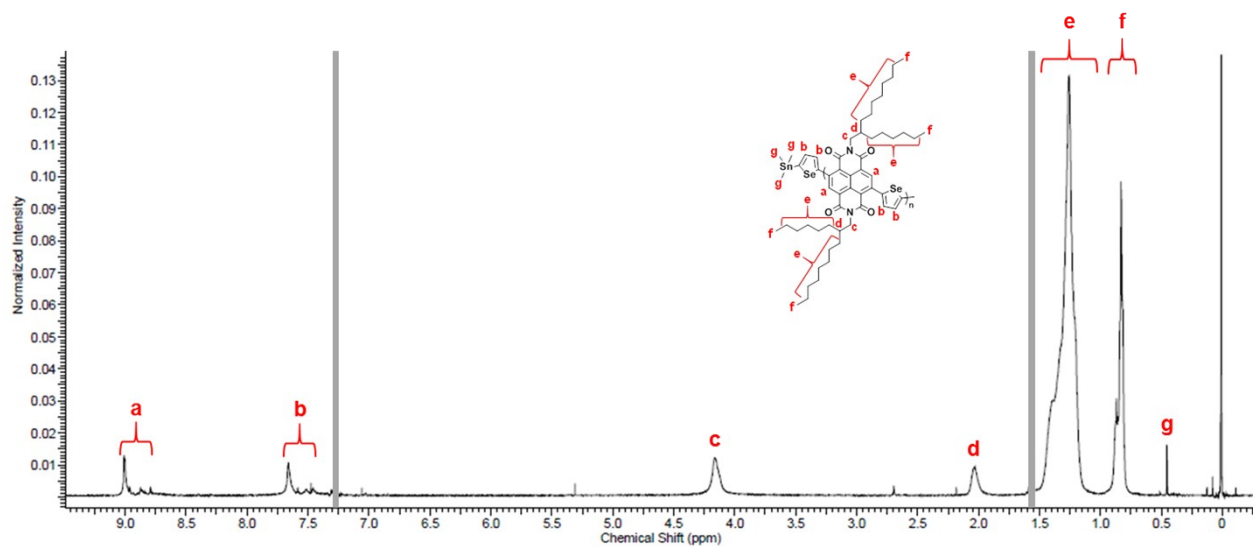


Fig S2. ^1H NMR spectrum of P2.

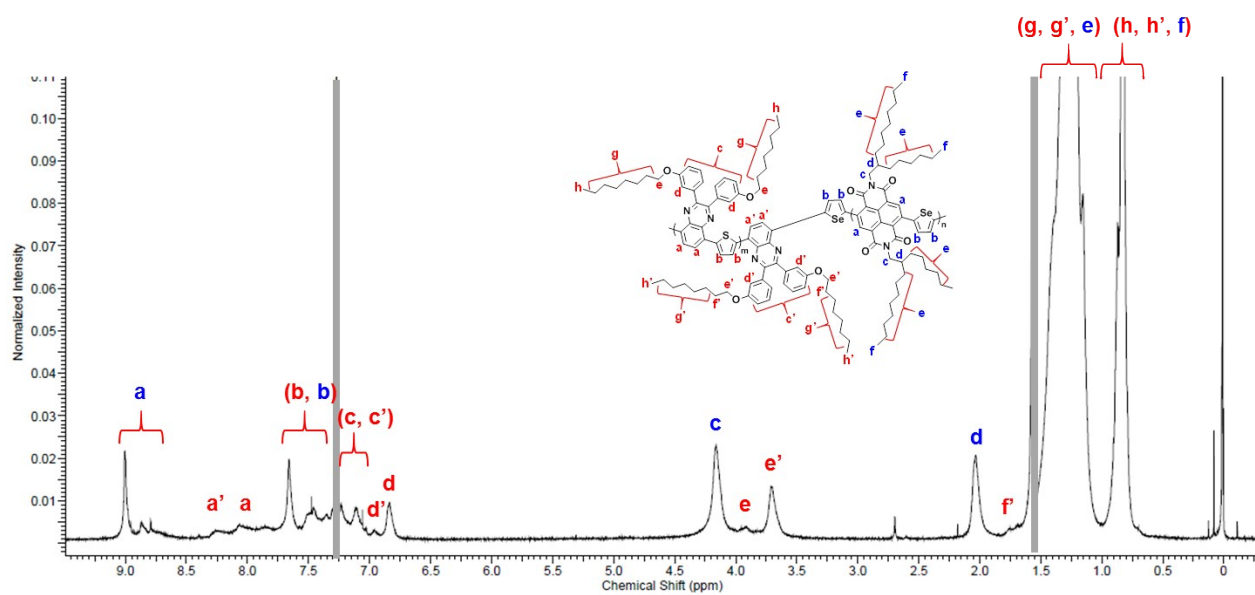


Fig S3. ^1H NMR spectrum of PTQI-*b*-PNDIS.

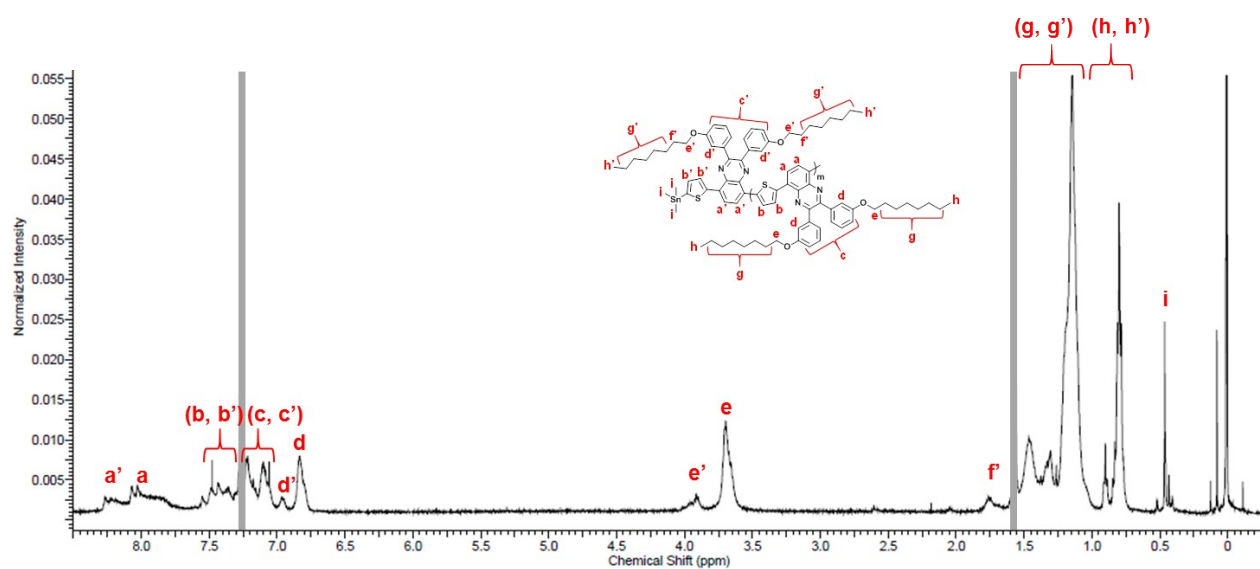


Fig S4. ^1H NMR spectrum of P3.

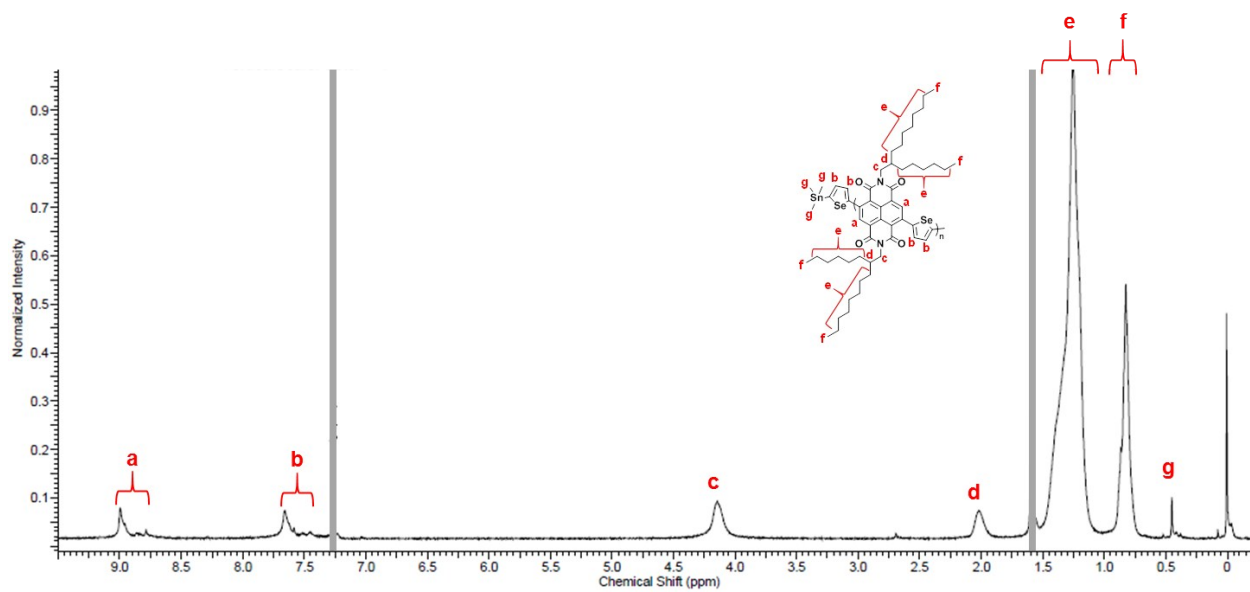


Fig S5. ^1H NMR spectrum of P4.

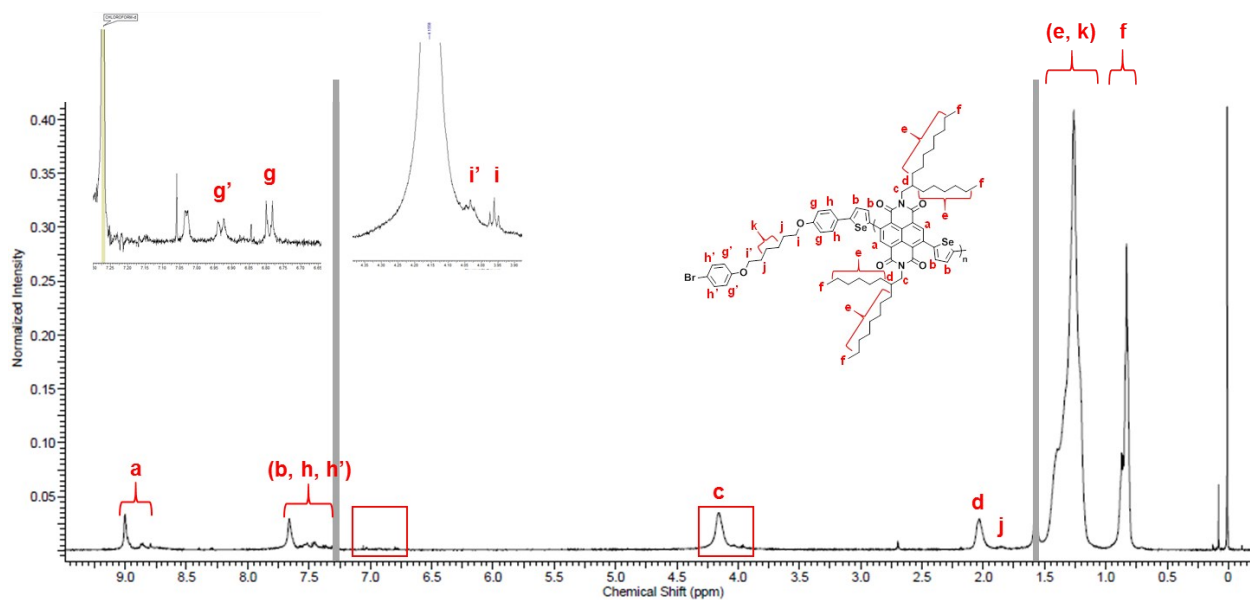


Fig S6. ^1H NMR spectrum of P5.

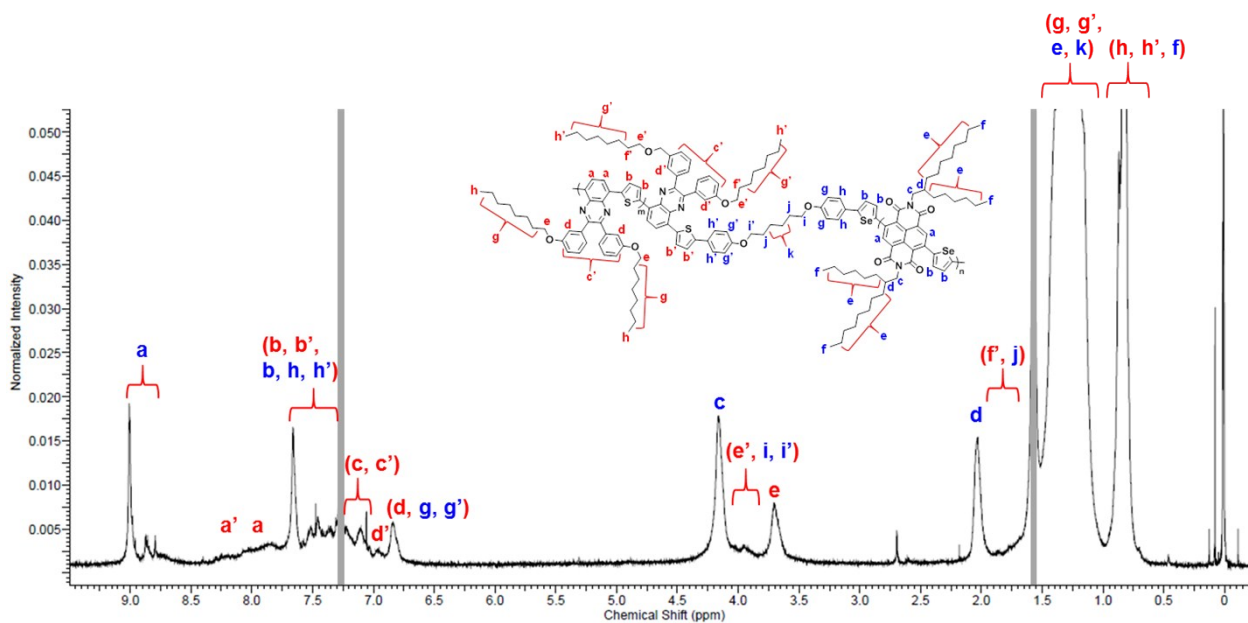


Fig S7. ¹H NMR spectrum of PTQI-*b*-PNDISL.

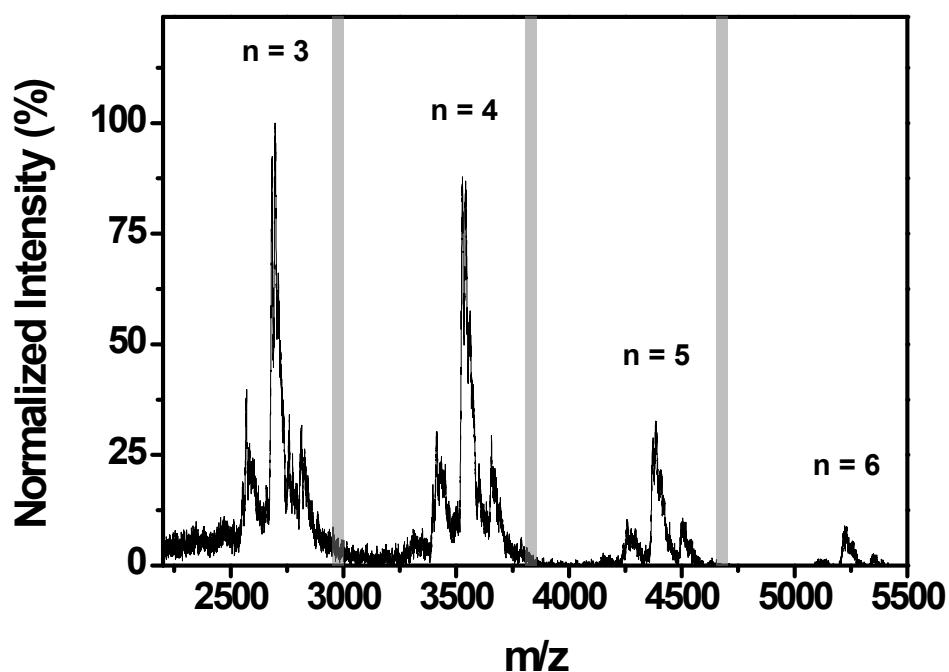


Fig S8. MALDI-TOF Mass spectrum of P4.

The peak with the highest sensitivity was observed at around 2700 m/z and the peaks were observed at around 3540, 4385, and 5225 m/z. This means that P4 contains trimer, tetramer, pentamer and a small amount of hexamer. These m/z values indicate that

trimethyltin is tethered to only one side of the P4 polymer chain end. If the P4 contain two trimethyltin groups at both ends, the peaks at around 2984, 3824, and 4666 m/z (gray area) should be observed. However, no peak appeared in those regions; therefore, bifunctionalized P4 does not exist.

Table S2. Molar ratios of repeating units, molecular weights, and polydispersity indices (PDIs) for the studied polymers.

	Molar ratio of repeat unit	M_n (g/mol)	M_w (g/mol)	PDI
P1	100/0	4952	7172	1.45
P2	0/100	7552	14284	1.89
PTQI- <i>b</i> -PNDIS	50/50	12425	26320	2.12
P3	100/0	3869	5204	1.35
P5	0/100	7590	15059	1.98
PTQI- <i>b</i> -PNDISL	50/50	11859	26377	2.22

Table S3. Optical and electrochemical properties of the block copolymers.

	Solution $\lambda_{\text{peak}}^{\text{abs}}$ (nm)	Film $\lambda_{\text{peak}}^{\text{abs}}$ (nm)	Solution $\lambda_{\text{peak}}^{\text{em}}$ (nm)	$\lambda_{\text{cut off}}^a$ (nm)	$E_g^{\text{opt } a}$ (eV)	Energy Levels	
						HOMO (eV) ^b	LUMO (eV) ^b
PTQI- <i>b</i> - PNDIS	564	619	646	728	1.70	-5.53	-3.83
PTQI- <i>b</i> - PNDISL	569	620	649	733	1.69	-5.50	-3.80

^a Film. ^b The values were obtained from cyclic voltammetry.

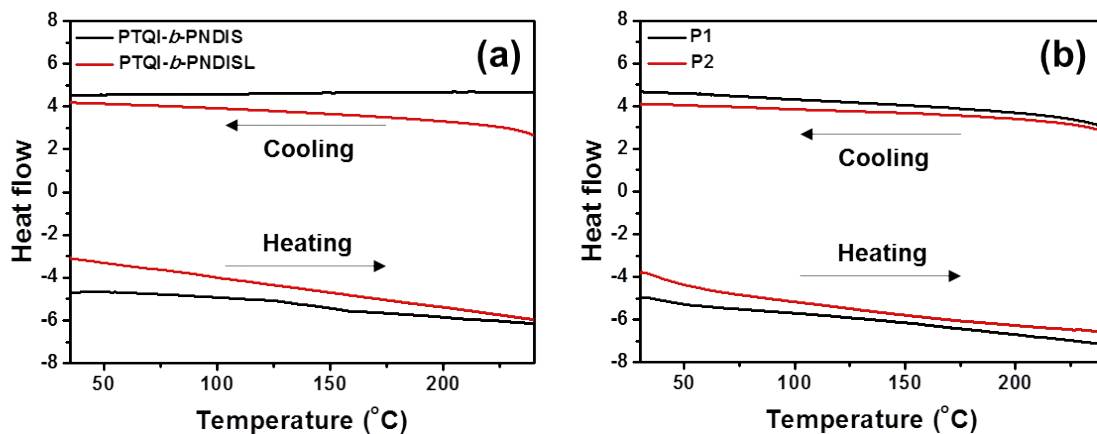


Fig S9. Differential scanning calorimetry (DSC) thermograms of (a) block copolymers and (b) P1 and P2.

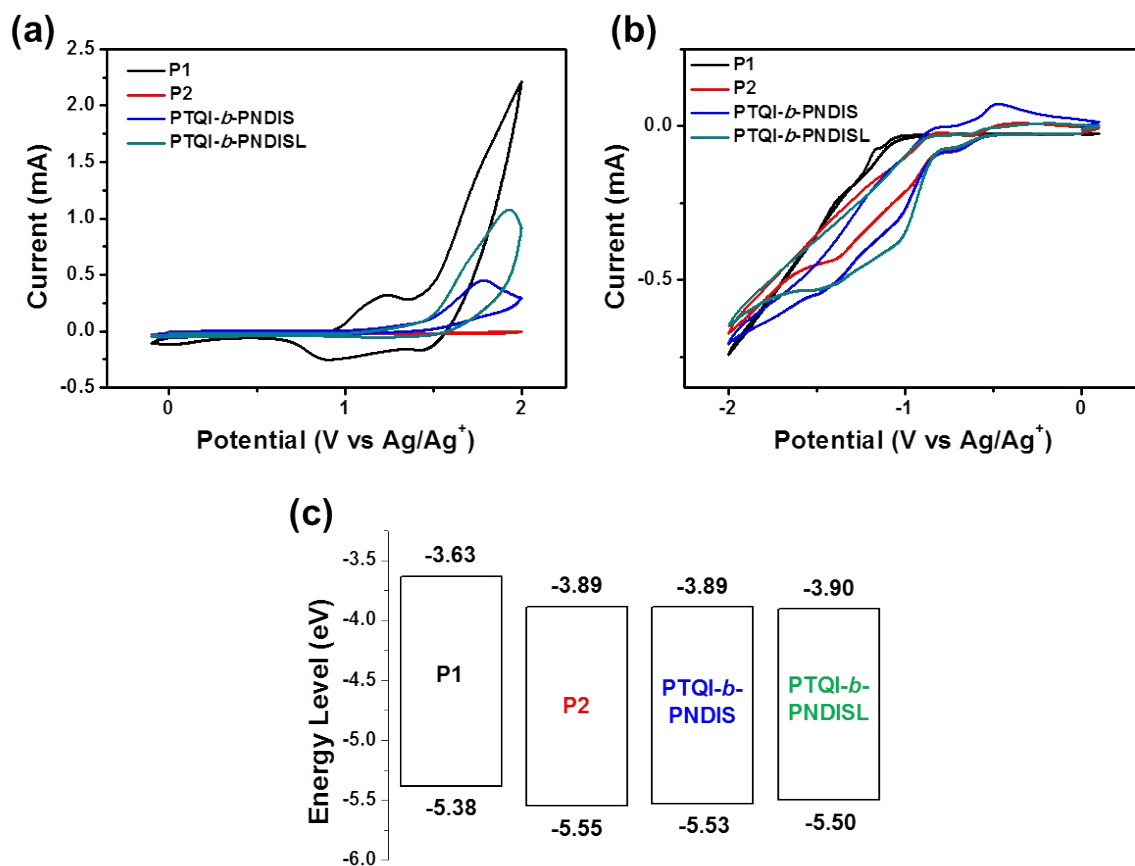


Fig S10. Oxidation (a) and reduction potentials (b) of P1, P2, PTQI-*b*-PNDIS, and PTQI-*b*-PNDISL films determined by cyclic voltammetry. (c) Energy diagram of P1, P2, PTQI-*b*-PNDIS, and PTQI-*b*-PNDISL films.

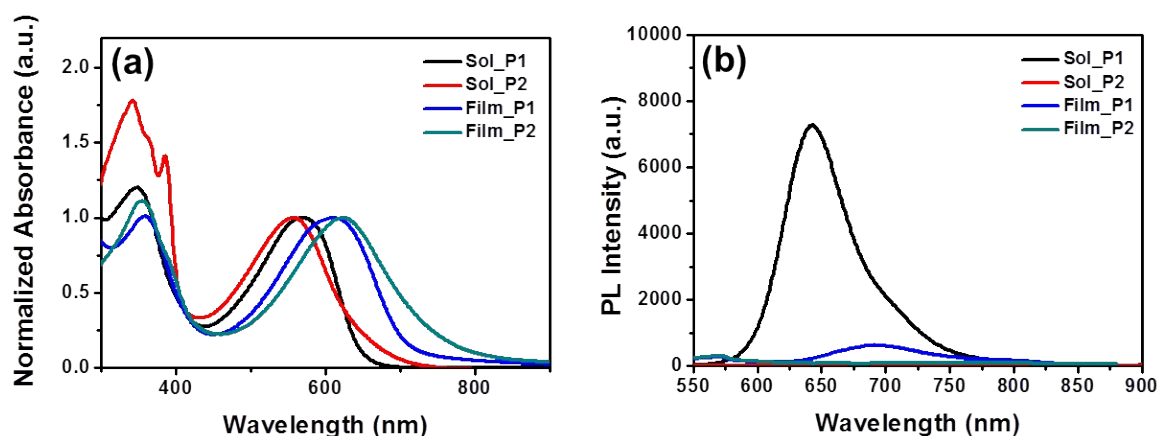


Fig S11. (a) UV-vis absorption spectra and (b) PL spectra of solution and films of P1 and P2.

Table S4. Optical and electrochemical properties of P1 and P2.

	M_n^a (kDa)	PDI	Solution	Film	Solution	Film	$\lambda_{\text{cut off}}^b$ (nm)	$E_g^{\text{opt } b}$ (eV)	Energy Levels	
			$\lambda^{\text{abs peak}}$ (nm)	$\lambda^{\text{abs peak}}$ (nm)	$\lambda^{\text{em peak}}$ (nm)	$\lambda^{\text{em peak}}$ (nm)			HOMO (eV)	LUMO (eV)
P1	5.0	1.45	569	612	643	693	707	1.75	-5.38 ^c	-3.63 ^d
P2	7.6	1.89	557	625	-	-	745	1.66	-5.94 ^e	-4.28 ^c

^a Determined by gel permeation chromatography and reported as their polystyrene equivalents. ^b Film. ^c The values obtained from cyclic voltammogram. ^d HOMO(eV) + E_g^{opt} (eV). ^e LUMO(eV) – E_g^{opt} (eV).

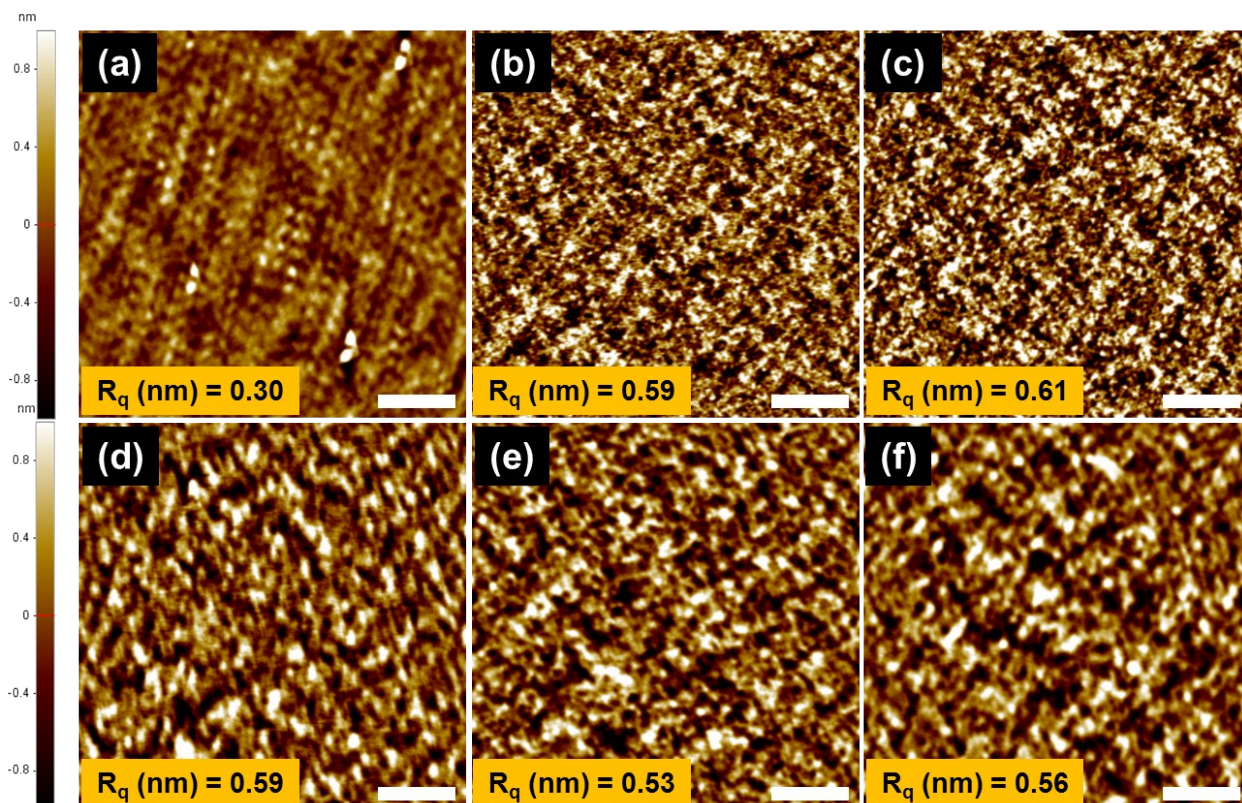


Fig S12. Surface topography AFM images (Scale bar = 1 μm) of the films. As-cast films: (a) blend of P1 and P2, (b) PTQI-*b*-PNDIS, and (c) PTQI-*b*-PNDISL. Annealed films: (d) blend of P1 and P2, (e) PTQI-*b*-PNDIS, and (f) PTQI-*b*-PNDISL. *The films were all thermally annealed at 200 $^{\circ}\text{C}$.

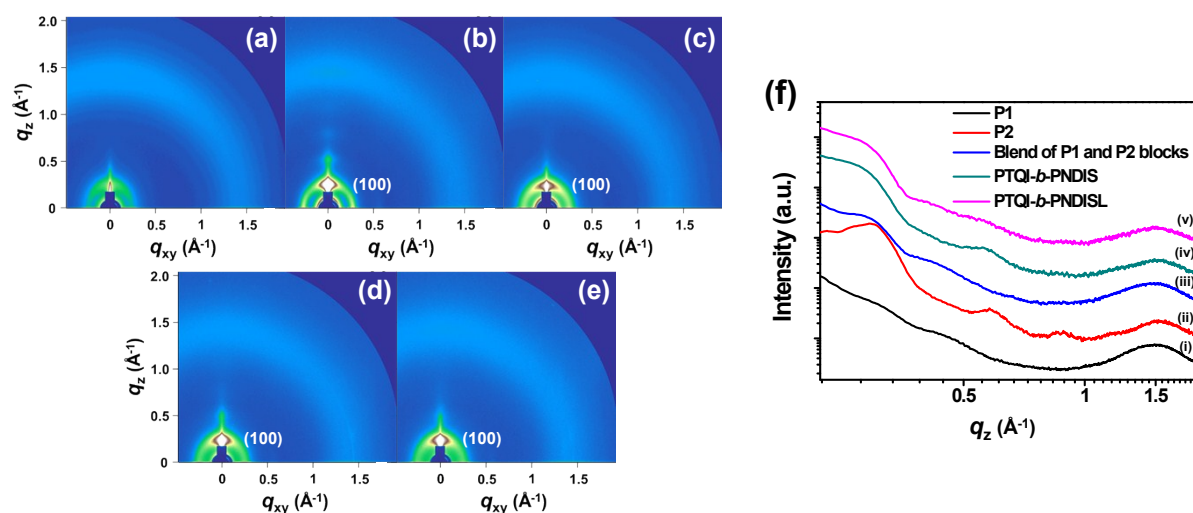


Fig S13. GIWAXS patterns as-cast films: (a) P1, (b) P2, (c) blend of P1 and P2, (d) PTQI-*b*-PNDIS, and (e) PTQI-*b*-PNDISL. (f) Out-of-plane GIWAXS patterns: As-cast films of (i) P1, (ii) P2, (iii) a P1 and P2 blend, (iv) PTQI-*b*-PNDIS, and (v) PTQI-*b*-PNDISL.

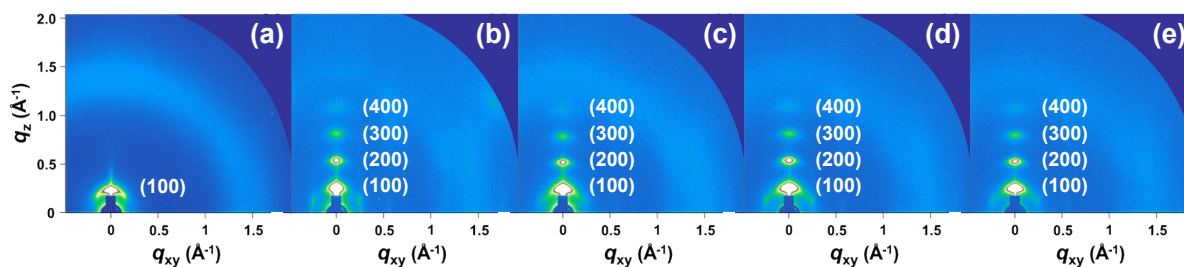


Fig S14. GIWAXS patterns annealed films: (a) P1, (b) P2, (c) blend of P1 and P2, (d) PTQI-*b*-PNDIS, and (e) PTQI-*b*-PNDISL. *The films were all thermally annealed at 200 °C.

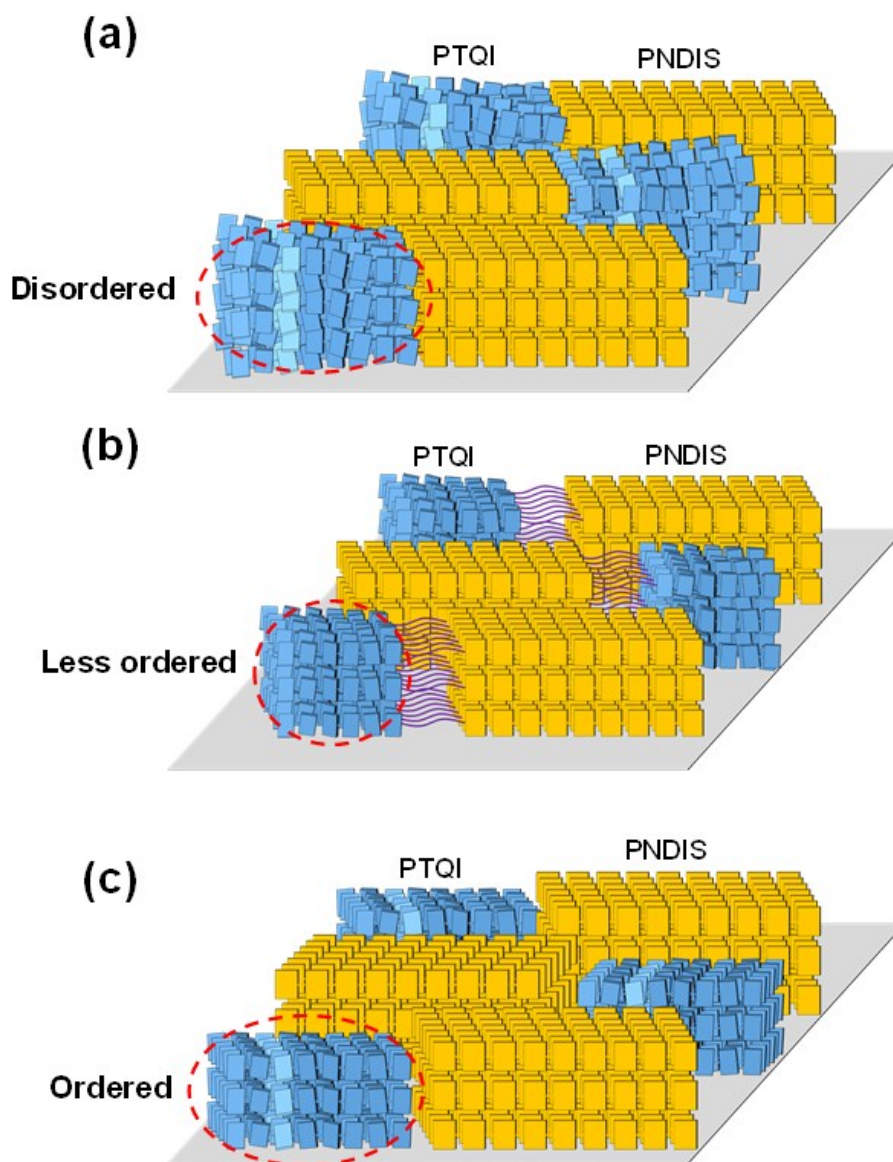


Fig S15. Expected possible schematic packing diagrams of (a) PTQI-*b*-PNDIS (disordered PTQI), (b) PTQI-*b*-PNDISL (less ordered PTQI), and (c) blend of P1 and P2 (ordered PTQI).

Table S5 Crystallographic parameters calculated from GIWAXS profiles of each block, a P1 and P2 blend, PTQI-*b*-PNDIS, and PTQI-*b*-PNDISL after thermal annealing.

Lamellar spacing (h00)	Out-of-plane		
	q_z (\AA^{-1})	d_{100} (\AA)	FWHM (\AA^{-1})
P1	0.251	24.98	0.0278
P2	0.277	22.66	0.0362
Blend of P1 and P2	0.267	23.50	0.0301
PTQI- <i>b</i> -PNDIS	0.283	22.18	0.0294
PTQI- <i>b</i> -PNDISL	0.275	22.83	0.0276

Table S6. The performance of PSCs made with blend of P1 and P2, PTQI-*b*-PNDIS, and PTQI-*b*-PNDISL.

	J_{sc} (mA cm^{-2})	V_{oc} (V)	FF (%)	PCE (%)
Blend of P1 and P2	1.16	0.67	37.4	0.40
PTQI- <i>b</i> -PNDIS	1.30	0.79	35.0	0.36
PTQI- <i>b</i> -PNDISL	4.04	0.79	48.1	1.54

* Additive solvent: DIO 3 vol%, thermal annealing at 80 °C for 10 min.

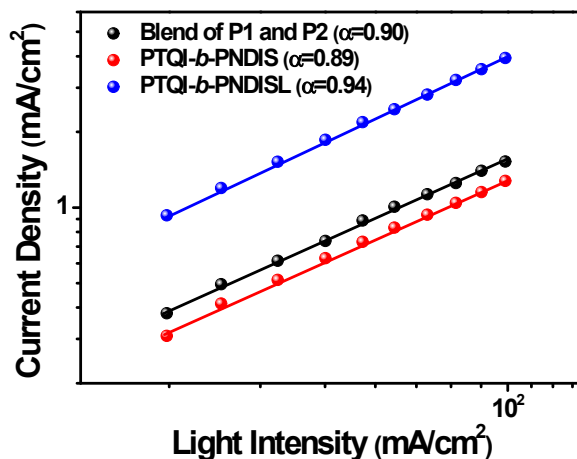


Fig S16. Incident light intensity vs. J_{sc} of PSCs made from the conjugated block copolymers and blend of P1 and P2: (black) blend of P1 and P2, (red) PTQI-*b*-PNDIS, and (blue) PTQI-*b*-PNDISL. *Solvent additive: DIO 3 vol%, thermal annealing at 80 °C for 10 min.

The power-law dependence of J_{sc} upon the incident light intensity can generally be expressed as $J_{sc} \propto P^\alpha$, where P is the light intensity and α is the exponential factor. If the value of α is close to unity, bimolecular recombination during the charge sweep-out under short-circuit conditions can be considered negligible.

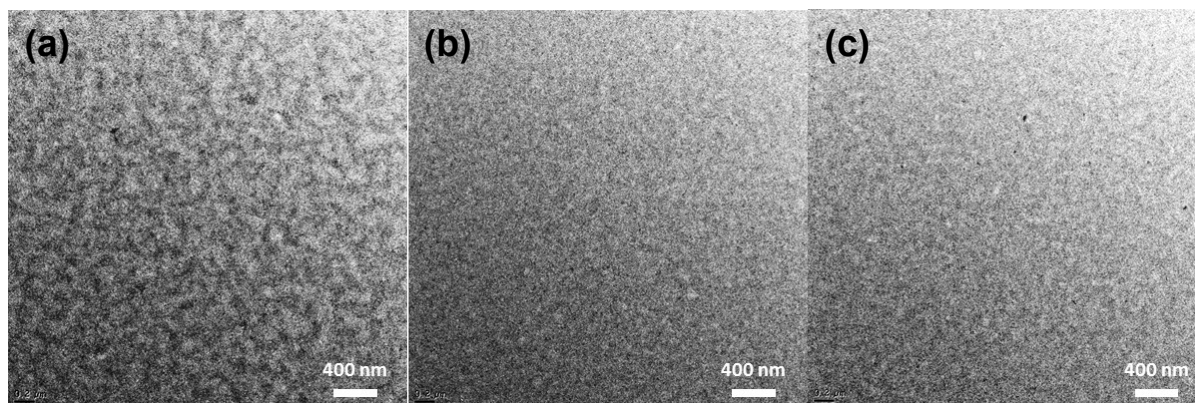


Fig S17. TEM images (Scale bar = 400 nm) of the active layer in PSC devices: (a) blend of P1 and P2, (b) PTQI-*b*-PNDIS, and (c) PTQI-*b*-PNDISL. *Solvent additive: DIO 3 vol%, thermal annealing at 80 °C for 10 min.

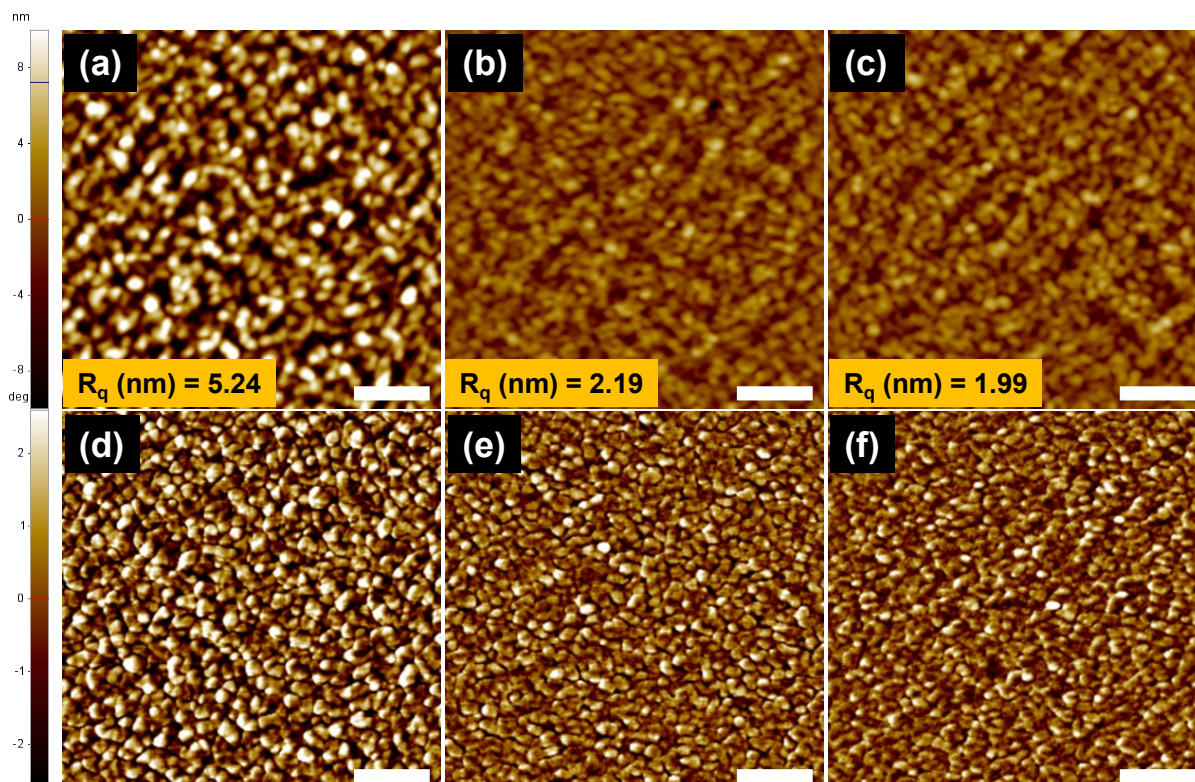


Fig S18. Surface topography and phase AFM images (Scale bar = 1 μm) of the active layer in PSCs: (a) blend of P1 and P2, (b) PTQI-*b*-PNDIS, and (c) PTQI-*b*-PNDISL. *Solvent additive: DIO 3 vol%, thermal annealing at 80 $^{\circ}\text{C}$ for 10 min.

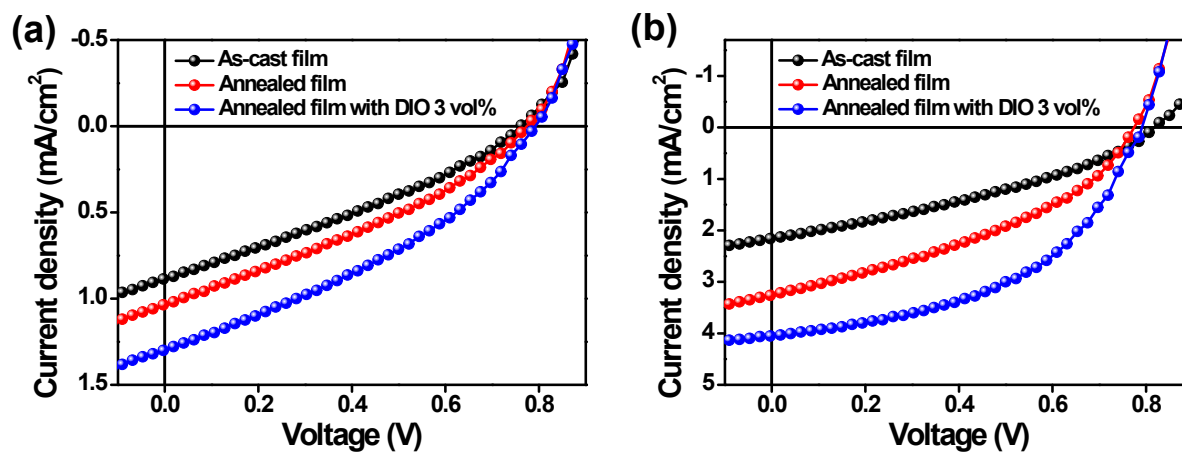


Fig S19. J - V characteristics of the PSCs fabricated from the block copolymer: (a) PTQI-*b*-PNDIS, (b) PTQI-*b*-PNDISL. (Black) As-cast, (red) annealed at 80 $^{\circ}\text{C}$ for 10 min, and (blue) block copolymer with DIO 3 vol% and thermally annealed at 80 $^{\circ}\text{C}$ for 10 min.

Table S7. The performance of PSCs made with the conjugated block copolymers under different conditions.

	Thermal annealing	Solvent additive	J_{sc} (mA cm ⁻²)	V_{oc} (V)	FF (%)	PCE (%)
	-	-	0.88	0.76	30.5	0.20
PTQI-<i>b</i>-PNDIS	80 °C 10 min	-	1.03	0.77	32.1	0.26
	80 °C 10 min	DIO 3 vol%	1.30	0.79	35.0	0.36
	-	-	2.16	0.84	33.4	0.60
PTQI-<i>b</i>-PNDISL	80 °C 10 min	-	3.25	0.78	38.0	0.96
	80 °C 10 min	DIO 3 vol%	4.04	0.79	48.1	1.54

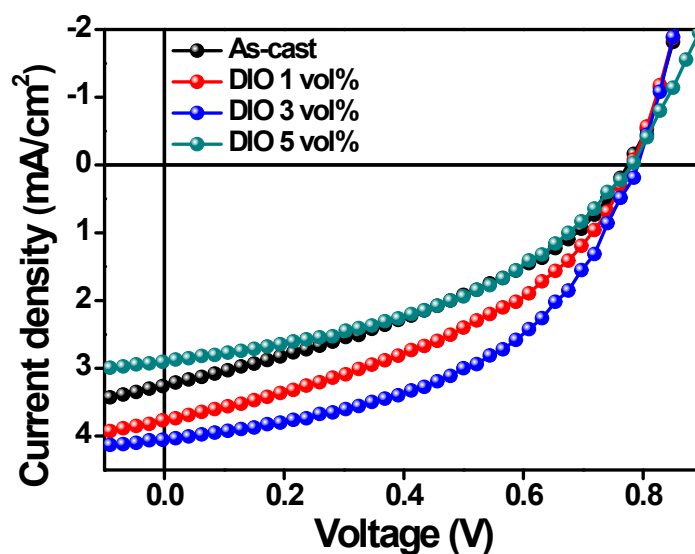


Fig S20. J - V characteristics of PSCs fabricated with PTQI-*b*-PNDISL: (black) As-cast, (red) DIO 1 vol%, (blue) DIO 3 vol%, (Green) DIO 5 vol%. *Thermal annealing at 80 °C for 10 min.

Table S8. The performance of PSCs made with PTQI-*b*-PNDISL under different conditions.

	Solvent additive	J_{sc} (mA cm ⁻²)	V_{oc} (V)	FF (%)	PCE (%)
	-	3.25	0.78	38.0	0.96
PTQI-<i>b</i>-PNDISL	DIO 1 vol%	3.76	0.78	40.8	1.20
	DIO 3 vol%	4.04	0.79	48.1	1.54
	DIO 5 vol%	2.89	0.78	42.9	0.97